Differential expression of speckled POZ protein, SPOP: Putative regulation by *miR-145*

Chiu-Jung Huang[1,2], Hsing-Yu Chen[3], Wan-Yi Lin[1,2] and Kong Bung Choo[4,5,*]

[1]*Department of Animal Science and* [2]*Graduate Institute of Biotechnology, Chinese Culture University, Yang Ming Shan, Taipei, Taiwan 111*

[3]*Graduate Program, Department of Biotechnology and Laboratory Science in Medicine, National Yang Ming University, Shipai, Taipei, Taiwan 112*

[4]*Department of Preclinical Sciences, Faculty of Medicine and Health Sciences and* [5]*Centre for Stem Cell Research, Universiti Tunku Abdul Rahman, Sg Long, Selangor, Malaysia*

**Corresponding author (Fax, 603-9019-7026; Email, chookb@utar.edu.my)*

The speckle POZ protein, SPOP, is an adaptor of the Cul3-based ubiquitination process, and has been implicated in the carcinogenesis process. Despite recent elucidation of biological functions, regulation of *SPOP* gene expression has not been reported. In this study, the mRNA levels of the mouse *SPOP* (*mSPOP*) gene were first shown to vary noticeably in different tissues. However, the SPOP protein was detected in high abundance only in Purkinje cells of the cerebellum and seminiferous tubule of the testis, echoing previous reports of involvement of ubiquitination in neuron cells and in spermatogenesis. In other mouse tissues and human cancer cell lines analysed, only low SPOP protein levels were detected. The 3′-untranslated regions of both the *mSPOP* and human *SPOP* transcripts harbor a conserved putative *miR-145* binding site (BS). In some tissues and cell lines, *miR-145* and SPOP protein levels were in an inverse relationship suggesting *miR-145* regulation. Luciferase assays of deletion and point mutation constructs of the *miR-145* BS, and *miR-145* induction by serum starvation that resulted in reduced endogenous SPOP levels provided further evidence that *miR-145* is likely involved in post-transcriptional regulation of SPOP expression in selected tissues, and possibly with the participation of other miRNA species.

[Huang C-J, Chen H-Y, Lin W-Y and Choo KB 2014 Differential expression of speckled POZ protein, SPOP: Putative regulation by *miR-145*. *J. Biosci.* **39** 401–413] **DOI** 10.1007/s12038-014-9432-1

1. Introduction

SPOP is a TRAF domain (TD)- and POZ-containing nuclear speckle-associated protein belonging to the TD/POZ protein family (Huang *et al.* 2004). SPOP has been reported to participate in many biological functions. SPOP is also called PDX-1 C-terminus-interacting factor 1, PCIF1, for its role in interacting with the C-terminus of pancreatic duodenal homeobox 1 (PDX-1) factor interfering with normal pancreas development (Liu *et al.* 2006). Besides PDX-1, SPOP has further been shown to regulate other transcriptional factors important to pancreas development (Claiborn *et al.* 2010). Human SPOP (hSPOP) was shown to be expressed in high levels in renal cell carcinomas; hSPOP overexpression and co-treatment with tumour necrosis factor (TNF) of HEK293 embryonic kidney cells increased the expression of the

Keywords. Cerebellar Purkinje cells; spermatogenesis; SPOP; miR-145; TD/POZ protein family; testicular seminiferous tubule

Abbreviations used: BS, binding site; MacroH2A1, macrohistone H2A1; PDX-1, pancreatic duodenal homeobox 1; PCIF1, PDX-1 C-terminus-interacting factor 1; PIPKIIβ, phosphatidylinositol phosphate kinase IIβ; Siah1A, seven-in-absentia homolog 1A; SPOP, speckled POZ protein; SRC-3, steroid receptor co-activator-3; TNF, tumour necrosis factor; TRAF, TNF receptor-associated factor; Ube2i, ubiquitin-conjugating enzyme 2i

Published online: 1 May 2014

oncogenic P-JNK and P-c-Jun proteins, suggesting a role for hSPOP in regulating tumour growth (Liu *et al.* 2009). The best-characterised function of SPOP is its participation in the Cul3-based protein ubiquitination and degradation processes (Hernandez-Munoz *et al.* 2005). SPOP binds with Cul3 ubiquitin ligase through the POZ domain and interacts with substrate proteins via the TD domain to form an ubiquitin ligase complex (Kwon *et al.* 2006). The multiple substrates targeted by the Cul3-SPOP ubiquitin ligase complex include phosphatidylinositol phosphate kinase IIβ (PIPKIIβ), Daxx, PDX-1, MacroH2A1 and SPOP itself (Takahashi *et al.* 2002; Hernandez-Munoz *et al.* 2005; Bunce *et al.* 2008). By degradation of these regulatory proteins, SPOP participates directly or indirectly in many biological reactions. It has also been shown that the POZ domain of SPOP confers proapoptotic functions in HeLa cells (Byun *et al.* 2007). Some tumours carry mutations in the SPOP gene; the SPOP genomic locus has also been shown to harbour a high percentage of genomic loss or loss of heterozygosity in breast cancers (Kan *et al.* 2010; Berger *et al.* 2011). These reports further link SPOP to the carcinogeneis process. Since SPOP expression is shown to inhibit SRC-3-mediated oncogenic signalling and carcinogenesis, SPOP is now thought to act as a tumour suppressor (Li *et al.* 2011).

In our previous attempt to elucidate the evolution of the *SPOP* gene in relation to other members of the TD/POZ family, an evolutionary scheme was proposed in which an ancestral TD/POZ gene underwent two independent routes of evolution, *viz.* retrotransposition and segmental duplication, to generate the contemporary set of TD/POZ genes (Choo *et al.* 2010). The identification of a novel and uncharacterized SPOP-like paralog, designated as SPOPL, in the human and rodent genomes, has further led us to propose that SPOP has evolved through segmental duplication whereas other tissue-specific and developmentally regulated TD/POZ members of unknown biological functions are evolutionary products of retrotransposition (Choo *et al.* 2010). Different modes of evolution inevitably exert strong influences on the mode and patterns of regulation of gene expression.

Despite the many reports on the biological functions of the SPOP protein, studies on the regulation of SPOP expression are still lacking. *SPOP* mRNA has been shown to be expressed ubiquitously but in varied quantities in different tissues; however, SPOP expression at the protein level has not been reported (Liu *et al.* 2004, 2009). In this work, we aimed to elucidate the mechanism of regulation of *SPOP* gene expression. We report here that the SPOP protein is expressed in high abundance in the Purkinje cells of the cerebellum in the brain and in the seminiferous tubule of the testis, but in low levels in other mouse and human tissues and cell lines analysed. This finding suggests the involvement of SPOP, an ubiquitin ligase, in the ubiquitination process in the neuron cells and in spermatogenesis. Our expression analysis data further support post-transcriptional regulation of SPOP expression by *microRNA-145*(*miR-145*).

2. Materials and methods

2.1 *Cell lines and mice*

All the human cell lines were obtained from the American Type Culture Collections through the BioResource Collection and Research Centre, an agent for ATCC cell lines in Taiwan. Besides the ATCC-approved human cell lines, no human tissues were used throughout the study. Normal mouse tissues were obtained from ICR mice purchased from the Laboratory Animal Centre, National Yang Ming University, Taipei, Taiwan. This study was approved by the Institutional Animal Care and Use Committee (IACUC) of the Chinese Culture University. The animals were sacrificed according to the IACUC guidelines.

2.2 *Cellular RNA preparation and real-time RT-PCR*

Preparation of total RNA and reverse transcription (RT) were performed as previously described (Huang *et al.* 2009). The relative *SPOP* mRNA levels were quantified by real-time RT-PCR using the DyNAmo^{TM} Flash SYBR® Green qPCR kit (Finnzymes, Espoo, Finland) as described (Choo *et al.* 2011). Primers used in this study are listed in table 1a. The real-time PCR programme used was: pre-incubation at 50°C for 2 min; initial denaturation at 95°C for 7 min; and 45 cycles at 95°C for 10 s, 59°C for 15 s and 72°C for 30 s. The reaction was terminated after a final extension at 60°C for 1 min and cooling at 40°C for 5 min. The relative *SPOP* mRNA levels were normalised to the mRNA level of the reference β-actin gene.

2.3 *Real-time RT-PCR for miRNA*

For miRNA analysis, total RNA was used and was prepared as described above. Polyadenylation was first performed using 500 ng RNA mixed with 2.5 μL 5X miRNA Reaction Buffer, 1.25 μL 25 mM $MnCl_2$, 0.5 μL 1 mM diluted ATP and 0.25 μL polyA polymerase provided in the NCode^{TM} miRNA First-Strand Polyadenylation and cDNA Synthesis Kit (Invitrogen, Carlsbad, CA, USA). Samples were adjusted to 12.5 μL with RNase-free water and incubated at 37°C for 15 min. For cDNA synthesis, 4 μL polyadenylated RNA from the previous step was added to 1 μL annealing buffer and 3 μL universal RT primer (25 μM) of the NCode^{TM} kit. Samples were heated at 65°C for 5 min and then cooled on

Table 1. Oligonucleotides used in this study

Oligonucleotide	Sequence
a. Real-time RT-PCR primers	
hSPOP F	5′- GTTCTACATTTTCATCAGGAGC -3′
hSPOP R	5′- GTAAAGTGACAGGTAATCTTTGC -3′
hβ-actin F	5′- GACCCAGATCATGTTTGAGACC -3′
hβ-actin R	5′- CTTCATGAGGTAGTCAGTCAGG -3′
mSpop F	5′- GAAGACGCAGGCAGTTGATTTC -3′
mSpop R	5′- ACGGTATGCTTCTGCCACTAAG -3′
mβ-actin F	5′- CCCTAAGGCCAACCGTGAAA AGAT -3′
mβ-actin R	5′- GTCTCCGGAGTCCATCACAATG -3′
miR-145 F	5′- GTCCAGTTTTCCCAGGAATCCCT -3′
Human U6 F	5′- CACCACGTTTATACGCCGGTG-3′
Mouse U6 F	5′- TCGCTTCGGCAGCACATA -3′
b. Oligonucleotides used for plasmid construction	
3′-UTR F	5′-TCTCTAGATCCTGCTTGTTGTAAGA CTC-3′
3′-UTR-F1	5′-GATCTAGAGACTGAGCAGAACAAAT CGTC-3′
3′-UTR-F3	5′-AATCTAGATTTGATCTGGAAGATGA GTG-3′
3′-UTR-S1R	5′-GATCTAGAGACGATTTGTTCTGCTCA GT -3′
3′-UTR-S2R	5′-CATCTAGACAAACAGCTGAGCAATC TG -3′
3′-UTR-S3R	5′-ATTCTAGAATATCTAAAAACAGAGA ACC -3′
3′-UTR-LR	5′-CTTCTAGACTCCACATTTATGTCCC CTG-3′
S2-R	5′-ATTCTAGAATATCTAAAAACAGA GAACC-3′
miR145-mutF	5′-CTTTATTGGTGTTGAA***CCA***TGGAA AAAATAACTCATC-3′
miR145-mutR	5′-GATGAGTTATTTTTTCCA***TGG***TTCA ACACCAATAAAG-3′
miR-145 F	5′-CTAGAGGGGATTCCTGGGAAAACTG GAC-3′
miR-145 R	5′-CTAGGTCCAGTTTTCCCAGGAATCC CCT-3′

In (b), restriction sites used in cloning are underlined; in miR145-mutF and -mutR, the mutated nucleotides are shown in bold and in italics.

ice for 1 min. The following RT reaction reagents were prepared and added to each RNA/primer mixture: 10 μL 2X First-Strand Reaction Mix and 2 μL SuperScript™ III RT/RNaseOUT™ Enzyme Mix (Invitrogen). The mixture was incubated at 50°C for 50 min followed by heating at 85°C for 5 min. For real-time PCR reaction, cDNA samples were diluted 10-fold with ddH_2O. The PCR reaction components contained 2.5 μL cDNA, 12.5 μL Platinum® SYBR® Green qPCR SuperMix-UDG (Invitrogen), 0.5 μL 10 μM gene-specific primer and the universal qPCR primer provided in the kit, 0.5 μL ROX reference dye and the volume was adjusted to 25 μL by diethylpolycarbonate-treated H_2O. Real-time PCR reaction was performed in the ABI PRISM® 7900HT Real-Time PCR System (Applied Biosystems, Foster City, CA, USA). The real-time PCR programme was: pre-incubation at 50°C for 2 min; initial denaturation at 95°C for 2 min; and 40 cycles at 95°C for 15 s, and 60°C for 1 min. This programme was terminated by a dissociation stage at 60°C for 1 min. *U6* snRNA was used for normalization.

2.4 *Western blot analysis*

Preparation of total cell lysates from tissues or cell lines and Western blot analysis were performed as described (Huang *et al.* 2012).The normal human colon protein sample was purchased from Zyagen (San Diego, CA, USA). Anti-hSPOP antiserum was purchased from Santa Cruz Biotechnology (Santa Cruz, CA, USA). For quantification of protein expression, the western blot results were scanned and computed using the UN-SCAN-IT gel-Version 6.1 Software (Silk Scientific, Inc., Orem, Utah, USA).

2.5 *Immunohistochemistry analysis*

Immunohistochemical analysis was performed as described (Huang *et al.* 2012). In brief, tissues were fixed in 4% paraformaldehyde/PBS and embedded in paraffin before sectioning. Sections of 5 μm thickness were dewaxed in 3% H_2O_2 in Tris buffer for 5 min and rinsed in running tap water to remove excess H_2O_2 before being immersed in 1% non-fat milk in Tris. Sections were then incubated with the anti-SPOP antiserum (Santa Cruz Biotechnology), followed by treatment with Bond™ Polymer Refine Detection (Leica Biosystems Newcastle Ltd, Newcastle, UK) for visualization before mounting.

2.6 *Plasmid construction and site-directed mutagenesis*

For luciferase (Luc) assay, the pGL3-Control (Promega, Madison, WI, USA) vector was used. To map the *hsa-miR145* binding site, serial-deletion constructs were derived as follows: PCR products containing the full-length or truncated 3′-untranslated region (3′-UTR) of the *hSPOP* sequences were digested with XbaI before being inserted into pGL3-Control (Jennewein *et al.* 2010; Liao *et al.* 2010). The retained nucleotide sequences in the 3′-UTR of the *hSPOP* constructs are as follows: RS1, nucleotide (nt) 1650-1987;

RS2, nt1650-2434; RS3, nt1650-2616; RL, nt1650-3112; RS2-4, nt2301-2434 and RS2-5, nt1967-2434. RS2-4Mut and RS2-5Mut contained the same region as in RS2-4 and RS2-5 but with the specified mutations in the *miR-145* binding site. A*hsa-miR-145* perfect-match construct was generated by direct ligation of double-stranded synthetic oligonucleotides (table 1b) via the XbaI restriction sites. Site-specific mutations were performed using the Phusion™ Site-Directed Mutagenesis commercial kit (Finnzymes) as previously described (Choo *et al.*2011). The mutations were confirmed by sequencing.

2.7 *Transient transfection and luciferase assays*

Transient transfection was performed using the PLUS™ Reagent and Lipofectamine™(Invitrogen) as previously described (Huang *et al.* 2005a, b). Luciferase assays were performed 48 h post-transfection using the Dual-Luciferase Reporter 1000 Assay kit (Promega) as described(Choo *et al.* 2011).

2.8 *Transient transfection with pre-miRNA*

Pre-miRNA oligomers were purchased from Applied Biosystems (Carlsbad, CA, USA). For transient transfection, 6 µL 50 µM pre-miRNA oligomers was mixed with Lipofectamin 2000 (Invitrogen) for transfection into HCT116 cells cultured to 50% confluency. At the indicated post-transfection time points, cells were harvested for western blot analysis.

3. Results

3.1 *High SPOP protein levels in the brain and testis but not in other tissues*

To determine mSPOP protein levels in the mouse, total lysates prepared from mouse tissues were used in western blot analysis (figure 1A). The tissues analysed were brain, lung, heart, liver, kidney, stomach and testis. The results showed significant mSPOP protein levels only in the brain and the testis but the protein was barely detectable, or was absent, in the lung, liver, kidney and stomach (figure 1A). A lower molecular-weight band was clearly detected in the heart which could be a mSPOP isoform; the identity of this aberrant band was not further investigated. The expression of mSPOP in the brain and testis was further examined by immunohistochemistry (figure 1B). The results showed that mSPOP was most abundantly detected in the Purkinje cells of the cerebellum in the brain, which appeared to be diffuse and cytoplasmic in the immunohistochemical staining. In the testis, mSPOP was detected in the seminiferous tubule.In the kidney control, no mSPOP protein was detected, consistent with the western blot data. Taken together, our data indicate differential expression

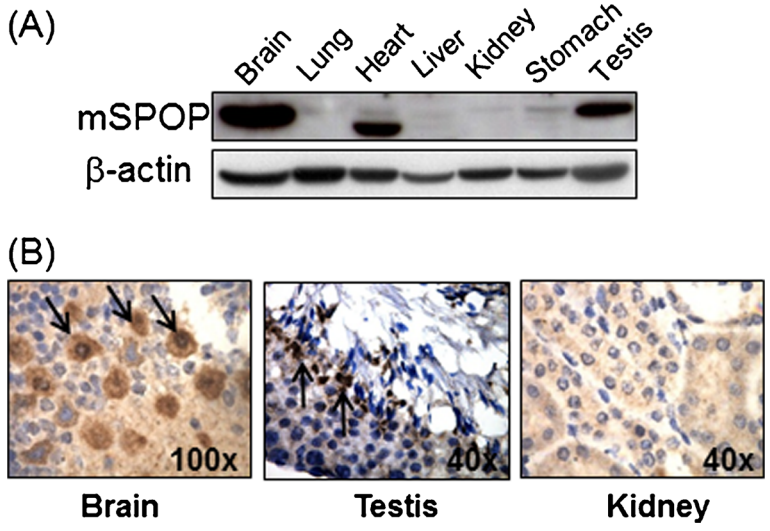

Figure 1. High abundance of mSPOP protein in Purkinje cells of the cerebellum and the seminiferous tubule of the testis. (**A**) Western blot analysis of mSPOP in mouse tissues using an anti-mSPOP serum. β-actin was used as the loading control. (**B**) Immunohistochemical detection of mSPOP in the mouse brain, testis and kidney. The arrow indicates mSPOP-positive Purkinje cells in the brain and in the spermatid in the seminiferous tubules of the testis.

of mSPOP protein in normal mouse tissues, and the brain and testis are the main sites of mSPOP expression.

3.2 *Discordant expression levels of the mSPOP protein and mRNA levels in mouse tissues*

To further investigate mSPOP expression, *mSPOP* mRNA levels in different mouse tissues were quantified by real-time RT-PCR, normalizing to a value of 1.0 arbitrarily assigned to the *mSPOP* mRNA level in the kidney (figure 2A). The results showed up to 23-fold differences in the *mSPOP* mRNA levels in different tissues, and the mRNA level was highest in the heart and lowest in testis. The relative mSPOP protein levels in the tissues described in figure 1A in the preceding section were quantified: up to 50-fold differences in them SPOP protein levels were observed between the kidney and the brain (figure 2B). However, the data did not seem to show concordance between the protein and mRNA levels in the tissues (figure 2), particularly in the testis in which the mRNA level was very low, whereas a significantly high mSPOP protein level was observed in this tissue. On the other hand, despite clear detection of mRNA, mSPOP protein

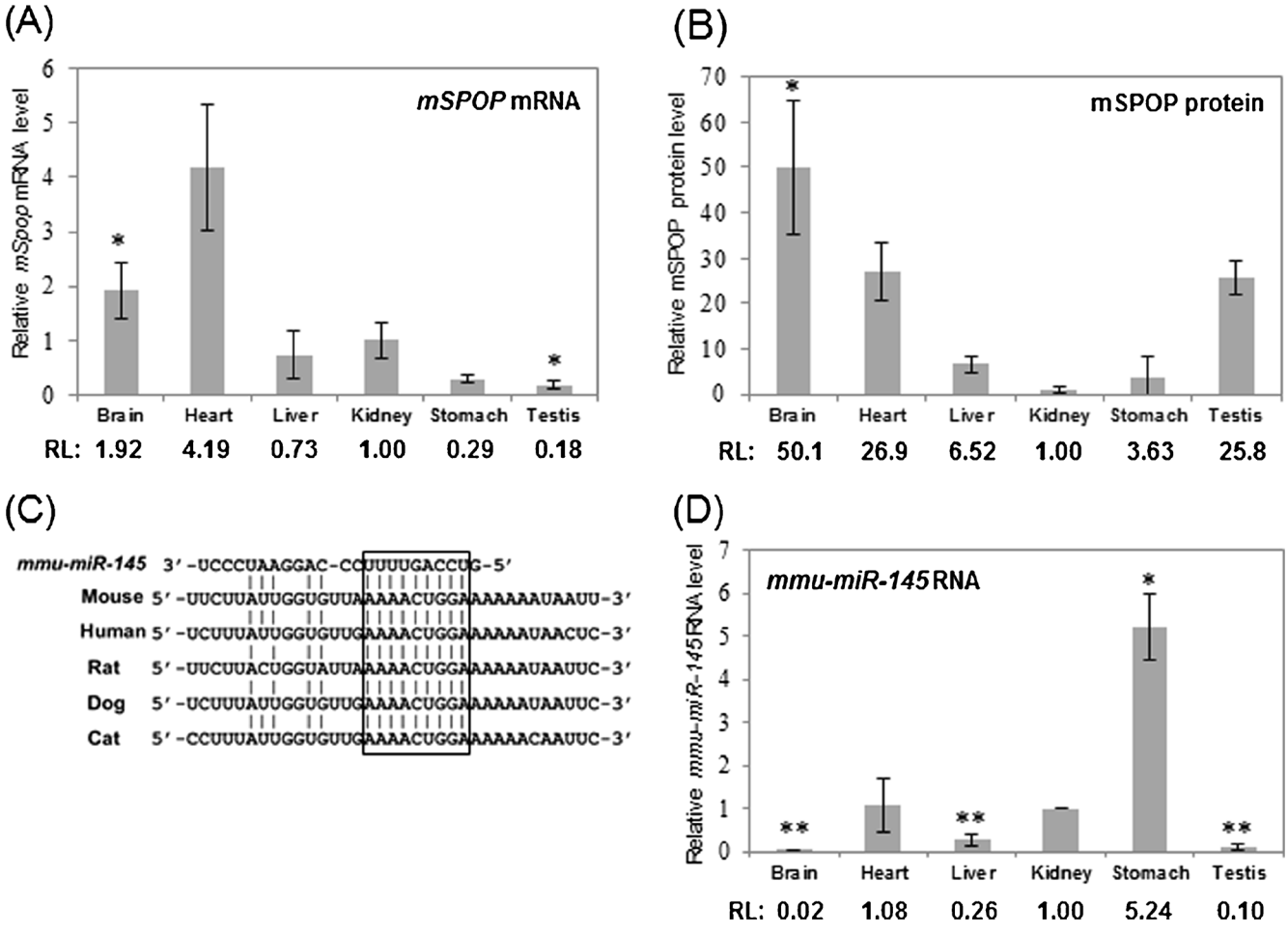

Figure 2. Discordant expression levels of the mSPOP protein and mRNA levels and differential levels of *mmu-miR-145* in the mouse tissues. (**A**) Quantification of the relative levels of *mSPOP* mRNA in the tissues by real-time RT-PCR. (**B**) The mSPOP protein levels as shown in figure 1A and derived in other experiments were quantified using β-actin as a normalization control. In both (**A**) and (**B**), the relative levels (RL) of mRNA or protein were computed using an arbitrary value of 1.0 assigned to the levels in the kidney. Data shown are the average of 3 independent experiments. *$p<0.05$ relative to the mRNA or protein level in the kidney. (**C**) Conservation of *mmu-miR-145* binding sequences in the mouse and other mammalian species. The seed sequence of *miR-145* is boxed. (**D**) Relative *mmu-miR145* levels (RL) in mouse tissues quantified by real-time RT-PCR using the *U6* RNA levels for normalization. Data shown are the average of 3 independent experiments. *$p<0.05$ and **$p<0.001$ relative to the *mmu-miR145* level in the kidney.

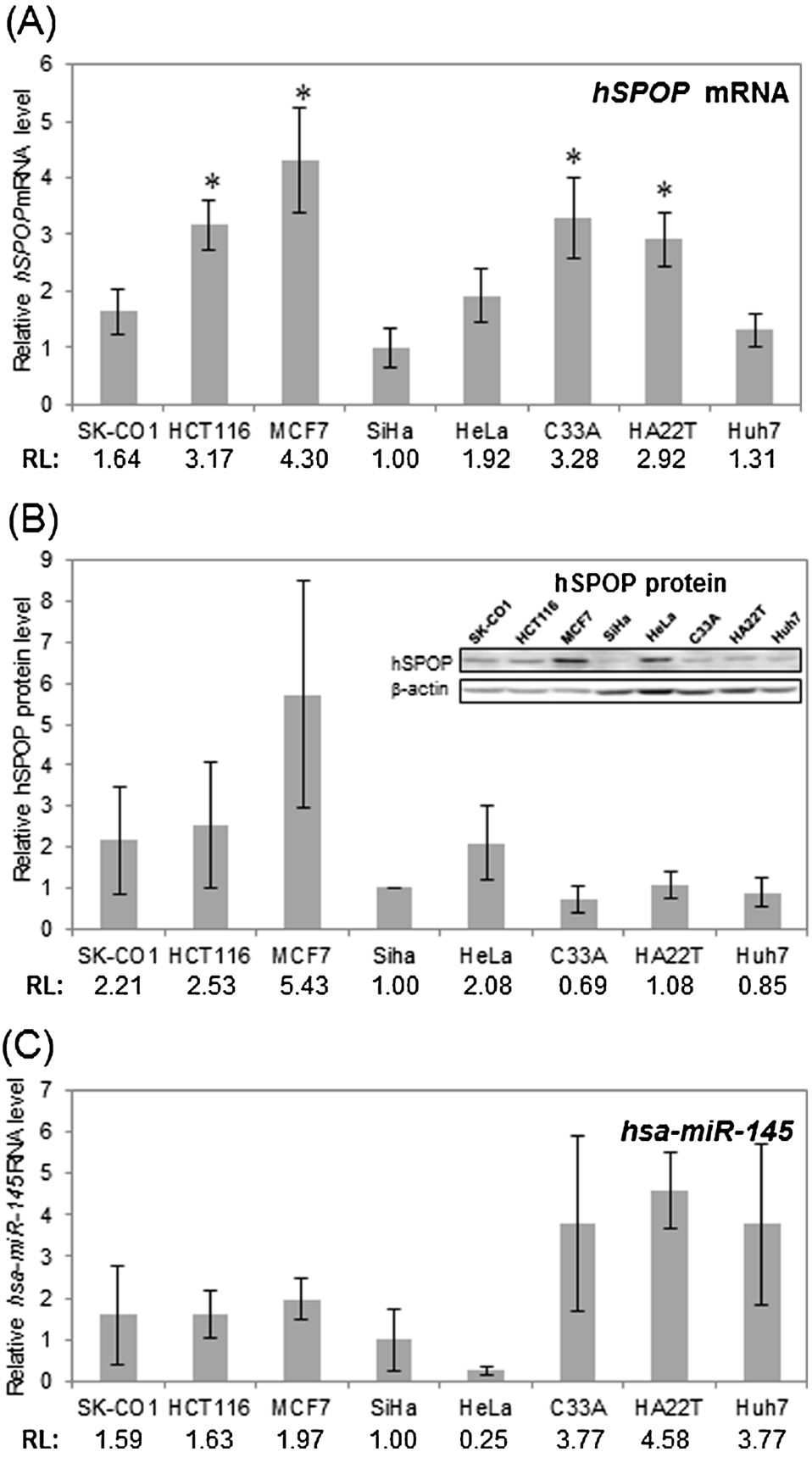
(A)
hSPOP mRNA
Relative hSPOPmRNA level
SK-CO1 HCT116 MCF7 SiHa HeLa C33A HA22T Huh7
RL: 1.64 3.17 4.30 1.00 1.92 3.28 2.92 1.31
(B)
hSPOP protein
Relative hSPOP protein level
hSPOP
β-actin
SK-CO1 HCT116 MCF7 Siha HeLa C33A HA22T Huh7
RL: 2.21 2.53 5.43 1.00 2.08 0.69 1.08 0.85
(C)
hsa-miR-145
Relative hsa-miR-145RNA level
SK-CO1 HCT116 MCF7 SiHa HeLa C33A HA22T Huh7
RL: 1.59 1.63 1.97 1.00 0.25 3.77 4.58 3.77

was barely detectable in the kidney. The discordant results between mRNA and protein levels, as also reported for other genes, suggest post-transcriptional regulation of *mSPOP* expression in these tissues.

3.3 *Inverse correlation between the expression levels of mSPOP protein and mmu-miR-145*

The *mSPOP* mRNA carries a long 3′-untranslated region (3′-UTR) of 1569 nucleotide (nt) in size, which constitutes about half the length of the *mSPOP* mRNA (data not shown). On interrogation of six miRNA databases, which included miRnada (Betel *et al.* 2008), PicTar (Krek *et al.* 2005), Targetscan (Friedman *et al.* 2009), PITA, DIANA and miRDB, a putative *mmu-miR-145* binding site, designated as mmu-miR-145BS, was predicted by all six databases (figure 2C). Further analysis showed conservation of a 9 nt seed sequence of the miRNA in the mammalian species examined (figure 2C, boxed sequences). To obtain experimental evidence on *mmu-miR-145*-mediated *mSPOP* regulation, the *mmu-miR-145* levels in the mouse tissues were quantified by real-time RT-PCR (figure 2D). The *mmu-miR-145* expression levels showed significant differences in the tissues tested; the highest and the lowest levels were found in the stomach and the brain, respectively, with a 262-fold difference.

When the relative *mmu-miR-145* levels were examined in relation to the relative mSPOP protein levels in the tissues (figure 2), it is noted that the highest mSPOP protein levels in the brain and the testis (50.1 and 25.8, respectively; figure 2B) were clearly inversely correlated with the lowest *mmu-miR-145* levels (0.02 and 0.1, respectively; figure 2D) in the two tissues. On the other hand, the lowest mSPOP protein relative levels in the kidney and stomach (1.00 and 3.63, respectively) correlated with the highest *mmu-miR-145* expression levels (1.00 and 5.24, respectively) in these tissues. In the liver and heart, correlation between the protein and miRNA levels is not so clearly defined, inversely or otherwise. The observed inverse correlation between the mSPOP protein and *mmu-miR-145* levels suggests post-transcriptional regulation of *mSPOP* by *mmu-miR-145* in the brain and testis, and possibly in the kidney and stomach. The data also suggest possible participation of other *cis* element(s) in *mSPOP* regulation in other tissues.

3.4 *Inverse correlation between the expression levels of hSPOP protein and hsa-miR-145 in human cancer cell lines*

In the preceding sections of our study, we aimed to examine differential SPOP expression in different tissues. Due to ethical consideration and the unavailability of human tissues, mouse tissues were used. We next aimed to analyse SPOP expression in cancer cells.Since the human and mouse SPOP proteins are identical in sequences (Choo *et al.* 2010), and due to the fact that human cancer cell lines are more readily available and are better characterized than mouse cancer cell lines, subsequent analysis of human SPOP (hSPOP) expression was performed using well characterized and approved human cancer cell lines obtained from ATCC.Included in the study were two colon cancer cell lines, SK-CO1 and HCT116, one breast cancer cell line MCF7, three cervical cancer cell lines SiHa, HeLa and C33A and two hepatoma cell lines, HA22T and Huh7. The relative *hSPOP* mRNA levels in these cell lines were also established by real-time RT-PCR, and the results were normalized to an arbitrary value of 1.0 designated to SiHa (figure 3A). *hSPOP* mRNA levels were relatively constant with up to 4.3-fold variations in the cancer cell lines analysed; *hSPOP* mRNA levels were highest in MCF7 and lowest in SiHa. When the relative hSPOP protein levels in the human cancer cell lines were next established by western blot analysis, the highest hSPOP protein level was found in MCF7, HeLa, HCT116 and SK-CO1whereas other cell lines showed relatively lower hSPOP protein levels (figure 3B). On examination of possible relationship between the relative mRNA and protein levels, a direct correlation between the mRNA and protein levels was noted in SK-CO1, HCT116 and MCF7, suggesting transcriptional regulation. On the contrary, the relative high mRNA levels appeared to be inversely correlated with lower protein levels in HeLa, C33A, HA22T and Huh7 cells, suggesting post-transcriptional regulation.

As in the case of *mSPOP*, a *hsa-miR-145* binding site (hsa-miR-145BS) is similarly predicted in the 3′-UTR of the human *hSPOP* mRNA. The relative *hsa-miR-145* levels in the human cell lines were determined as for the mouse tissues, and the results were computed relative to an arbitrary value of 1.0 assigned to SiHa. Up to 18.3-fold difference in the *hsa-miR-145* levels was observed between HeLa and HA22T (figure 3C). When the *hsa-miR-145* levels were examined relative to the relative hSPOP protein levels, the lower protein levels in C33A, Huh7 and HA22T (0.69, 0.85

◀ **Figure 3.** Inverse correlation between the expression levels of the human SPOP protein and *hsa-miR-145* in human cancer cell lines. Quantification of the relative levels of *hSPOP* mRNA (**A**) and protein levels (**B**), and the *hsa-miR145* levels (**C**) is as described in figure 2 legend. In (**B**), a typical western blot was inserted. In all panels, the relative levels are presented using the arbitrary SiHa data as 1.0. Data shown were derived from 3 independent experiments. * $p<0.05$ relative to the SiHa level.

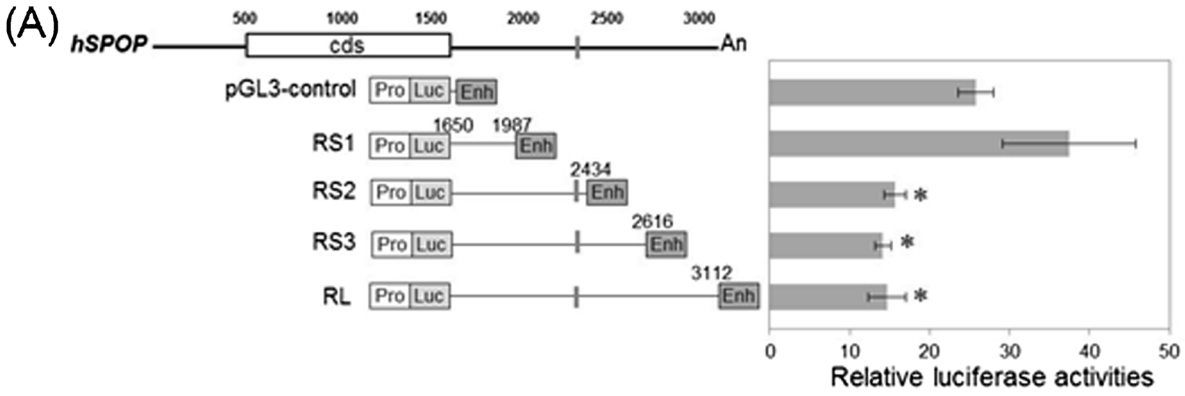
(A)
hSPOP
500
1000
1500
2000
2500
3000
cds
An
pGL3-control
Pro Luc Enh
RS1
1650
1987
RS2
2434
RS3
2616
RL
3112
0
10
20
30
40
50
Relative luciferase activities

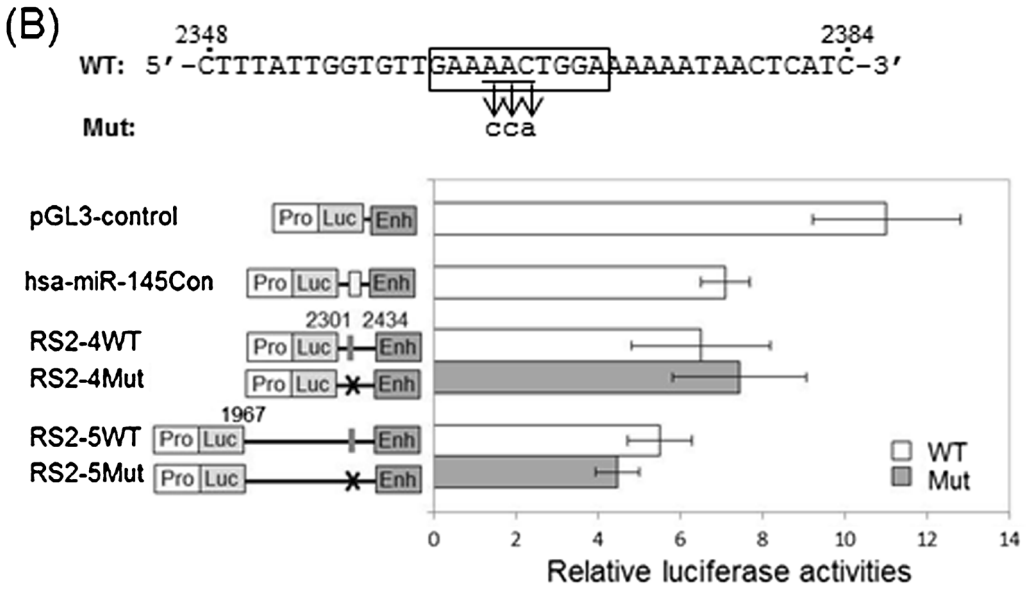
(B)
2348
2384
WT: 5′-CTTTATTGGTGTTGAAAACTGGAAAAAATAACTCATC-3′
Mut:
cca
pGL3-control
hsa-miR-145Con
2301 2434
RS2-4WT
RS2-4Mut
1967
RS2-5WT
RS2-5Mut
WT
Mut
0
2
4
6
8
10
12
14
Relative luciferase activities

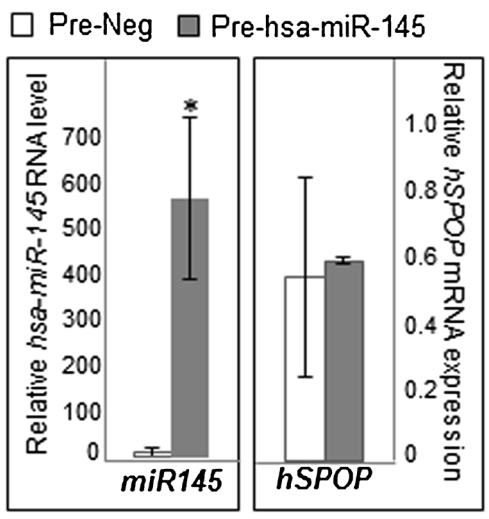
(C)
Pre-Neg
Pre-hsa-miR-145
Relative hsa-miR-145 RNA level
700
600
500
400
300
200
100
0
miR145
hSPOP
Relative hSPOP mRNA expression
1.0
0.8
0.6
0.4
0.2
0

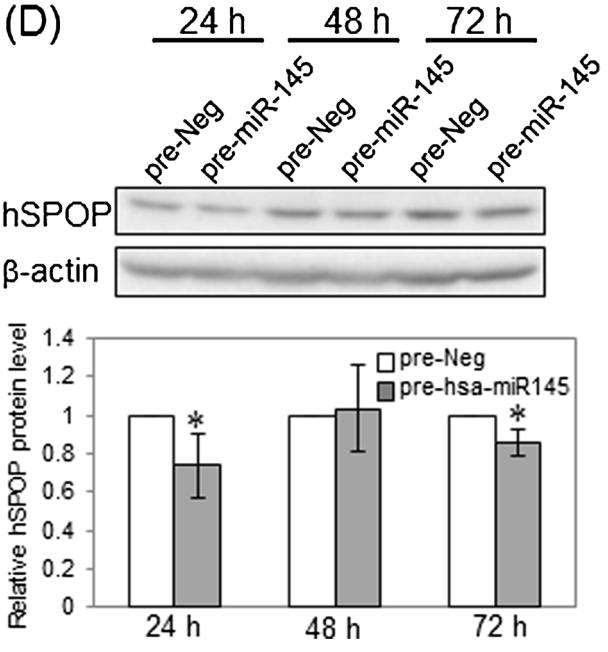
(D)
24 h
48 h
72 h
pre-Neg
pre-miR-145
hSPOP
β-actin
Relative hSPOP protein level
1.4
1.2
1
0.8
0.6
0.4
0.2
0
pre-Neg
pre-hsa-miR145
24 h
48 h
72 h

and 1.08, respectively) were inversely correlated with the higher *hsa-miR-145* levels (3.77, 3.77 and 4.58, respectively). Similarly, the relative higher hSPOP protein levels found in SK-CO1, HCT116 and MCF7 cells (2.21, 2.53 and 5.43, respectively) were also inversely correlated with the relatively lower *hsa-miR-145* levels (1.59, 1.63 and 1.97, respectively) in these cell lines, supporting post-transcriptional *SPOP* regulation by *miR-145* as first suggested in the analysis of the mouse *SPOP* gene above.

3.5 *Putative miR-145 binding site is possibly targeted by miR-145 in SPOP regulation*

To experimentally demonstrate *hsa-miR-145* repression of *hSPOP* expression, various lengths of the 3′-UTR sequence of *hSPOP*, with or without the putative hsa-miR-145BS, were cloned into the pGL3-control luciferase plasmid under the transcriptional regulation of the SV40 promoter and enhancer (Choo *et al.* 2011) (figure 4A). For selection of an optimal cell line for use in luciferase transfection assays, a number of cell lines, including HeLa and C33A (cervical cancer cell lines) and the HCT116 and SK-CO1 (colon cancer cells) were initially tested, and similar results were obtained (data not shown). For subsequent experiments, HCT116 cells were chosen because it is the colon cancer cell line that showed the highest SPOP protein level (MCF7 is a breast cancer cell line) and was, hence, easier to observe miRNA-regulated post-transcriptional regulation. Secondly, it is a cell line in which miRNA-145 is known to be up-regulated by serum starvation (Sachdeva *et al.* 2009), a fact that was subsequently exploited for the analysis of effects of *in vivo* alterations of miR-145 levels on SPOP (see below).

The luciferase constructs were transiently transfected into HCT116 cells, and the cells were harvested for luciferase assays two days post-transfection. When compared with the luciferase activity of the pGL3-control plasmid with no hSPOP sequence insertion, the inclusion of a 338-bp 3′-UTR insert in the construct RS1, which did not include the putative *hsa-miR-145* binding site, resulted in a 45.4% increase of luciferase activities relative to the no-insert control (figure 4A). On the other hand, all hsa-miR-145BS-containing constructs, RS2, RS3 and RL, showed 39.2%, 45.1% and 43.1%, respectively, significantly lower luciferase activities relative to RS1. The transient transfection results, therefore, support the presence of a *cis*-repressive sequence in the minimal 3′-UTR segment between nt 1987-2434 within which the putative hsa-miR-145BS is located. The results also suggest the presence of positive-acting *cis* element(s) in the nt 1987-24343′-UTR segment.

On alignment of the sequences of *hsa-miR-145* and the putative hsa-miR145BS, a 10 nt seed sequence is discernable (figure 4B, boxed WT sequence). For further luciferase assays, hsa-miR-145BS mutants were next created in the luciferase constructs R2-4 and R2-5 which harboured the minimal lengths of the *hSPOP* 3′-UTR sequence (figure 4B). When a construct, hsa-miR-145C, on containing the exact *hsa-miR-145* sequence, was used as a control in the transfection, the luciferase activities were reduced to 64.4% that of the insert-free pGL3-control plasmid, indicating targeting by endogenous *hsa-miR-145*. The luciferase activities of the wild-type constructs RS2-4WT and RS2-5WT were also reduced to 59.0% and 50.0%, respectively, that of pGL3-control, supporting similar *hsa-miR-145*-targeted suppression. When the hsa-miR-145BS was mutated in the minimal-length (134 bp) RS2-4Mut construct, the luciferase activities of the mutant were consistently higher than in the wild-type RS2-4WT construct, further indicating involvement of hsa-miR-145BS in regulating expression of

◀ **Figure 4.** Targeting of the putative *hSPOP* miRNA binding site by *hsa-miR145*. (**A**) Luciferase assays of transcriptional activities of 3′-untranslated region (UTR) of *hSPOP*. The top line shows the *hSPOP* mRNA sequence in which the open box and the line scheme represent the coding sequence (cds) and the 5′- and 3′-UTR of *hSPOP*, respectively. RS1, RS2, RS3 and RL plasmids were created by inserting different lengths of *hSPOP*3′-UTR between the luciferase (Luc) gene and the enhancer (Enh) of the pGL3-control vector. The thick vertical bars represent the putative *hsa-miR145* binding site in *hSPOP*. Boundaries of the 3′-UTR segments analysed are shown relative to the *hSPOP* mRNA sequence. The constructs were transfected transiently into HCT116 and luciferase activities were measured two days post-transfection. The relative activities of shown in the right panel are from three independent experiments.*$p<0.05$ relative to the empty pGL3-control. (**B**) Mutation analysis of the *hsa-miR-145* binding site in luciferase assays. On the top, the wild-type (WT) and the mutant (Mut) sequences around the miRNA BS are shown; the mutated nucleotides in the seed sequence (boxed) are indicated by arrows. The wild-type and mutant constructs were transfected into HCT116 cells for luciferase assays as in (**A**) above. A construct, hsa-miR-145Con, harbouring the perfect *hsa-miR-145* sequence, was used as a control. In the schematic display of the constructs, vertical bars indicate WT and crosses represent the mutation in the *hsa-miR145* BS. The data shown are from 3 independent transfection experiments. (**C**) Ectopic overexpression of *hsa-miR-145*. A precursor of *hsa-miR-145* (pre-miR-145) or a previously validated negative control of scrambled sequence (Pre-Neg) was transfected into HCT116 followed by real-time RT-PCR quantification of the relative *hsa-miR-145* in transfected cells. (**D**) Overexpression of *hsa-miR-145* decreased the endogenous hSPOP protein level. The pre-miR negative control (Pre-Neg) or pre-hsa-miR-145 precursor (Pre-hsa-miR-145) was transfected into HCT116 cells, respectively, and cells were harvested at 24 h, 48 h or 72 h post-transfection for mSPOP western blot analysis. A representative western blot is shown in the top panel; quantified results of three independent transfection experiments and western blot analyses are shown in the bottom panel. In all data presented, *$p<0.05$.

the reporter gene. However, when the hsa-miR-145BS was mutated in the longer (468-bp) RS2-5Mut construct, the luciferase activity was unexpectedly found to be further reduced relative to the wild-type construct, an observation that may be explained by the presence of other positive-acting *cis* element(s) in the 468-bp sequence preceding the hsa-miR-145BS.

Further and more direct evidence on putative *hsa-miR-145* regulation was sought by testing the effects of ectopic over-expression of *hsa-miR145* on endogenous hSPOP protein level in HCT116 cells. *hsa-miR-145* overexpression was achieved by transfection of a *hsa-miR-145* precursor, pre-hsa-miR-145, into HCT116 cells followed by hSPOP western blot analysis at various time points.On pre-hsa-miR-145 transfection, *hsa-miR-145* was shown to be elevated by 42-fold, whereas transfection of the previously validated Pre-Neg negative control with a scrambled sequence did not result in detectable increase in the *hsa-miR-145* level (figure 4C, left panel). The mRNA of *hSPOP* did not change significantly when cells transfected with pre-hsa-miR-145 (figure 4C, right panel). In comparison with data obtained by pre-Neg transfection, ectopic *hsa-miR-145* overexpression resulted in 26.2% and 14.1% significant reduction of hSPOP protein levels 24 h and 72 h post-transfection, although reduced hSPOP level was not evident at 48 h (figure 4D). These results are further evidences to support *miR-145*-mediated regulation of *SPOP* expression by translational repression in the cell lines analysed.

It has previously been reported that serum starvation significantly up-regulates *hsa-miR-145* expression levels in some cell lines through the *Akt* and TP53 pathways, and HCT116 was one such cell line tested (Sachdeva *et al.* 2009). HeLa and HCT116, which showed low and intermediate levels of *hsa-miR-145*, respectively, were cultured under serum starvation conditions as described by Sachdeva *et al.* Induction of *hsa-miR-145* was confirmed in HCT116 but no appreciable induction was detected in the HeLa cells (figure 5A). In contrast to an apparent increase in the *hSPOP* mRNA levels in the HeLa cells, serum starvation had no effects on the *hSPOP* mRNA level in HCT116 (figure 5B). More importantly, in both HeLa and HCT116, significant decreases in the endogenous hSPOP protein levels were demonstrated in the serum-starved cells (figure 5C). Taken together, *in vivo* induction of *hsa-miR-145* in HCT116 has resulted in down-regulation of endogenous hSPOP protein independent of changes in the mRNA levels, further supporting a possible role for *hsa-miR-145* in regulating *hSPOP* expression in the cell lines tested.

4. Discussion

In this study, the SPOP protein was shown to be present in high abundance in the Purkinje cells of the brain and the seminiferous tubule of the testis (figure 1B); in other tissues analysed, SPOP was only appreciably detectable. Cerebellar Purkinje cells are large dendritic neuron cells located in the cerebellum of the brain. One major mechanism that leads to neurodegenerative diseases, including Alzheimer's and Parkinson's diseases, is thought to be associated with dysfunctional ubiquitin-proteasome regulation leading to aggregation of ubiquitylated proteins into inclusion bodies and subsequent neuronal death (Huang and Figueiredo-Pereira 2010; Matsuda and Tanaka 2010). In a Purkinje cell GRP78/BiP-null knockout mouse model, cytosolic ubiquitinated proteins were dramatically reduced, leading to accelerate cerebellar degeneration (Wang *et al.* 2010). Seven-in-absentia homolog 1A (Siah1A) is another ubiquitin ligase that is highly expressed in the Purkunje cells to mediate ubiquitination and degradation of group 1 metabotropic glutamate receptors that are critical for neural plasticity in Purkinje cells (Moriyoshi *et al.* 2004). This is a first report of a new ubiquitin ligase, SPOP, being present in high abundance in the cerebellar Purkinje cells, further supporting important participation of the ubiquitination process in neuron cells.

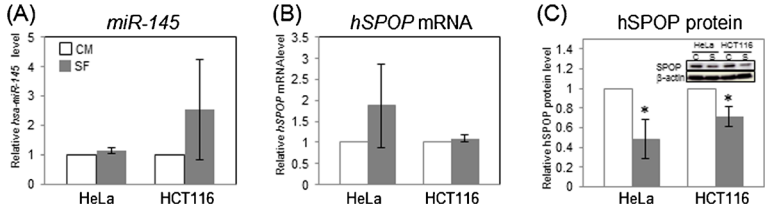

Figure 5. Serum starvation induces *hsa-miR-145* expression and down-regulates hSPOP protein levels. Cells were cultured either in complete medium (CM, open bar) with 10% fetal bovine serum, or without serum (SF, filled bar) for 24 h before the cells were harvested for analysis. (**A**) Induction of *hsa-miR-145* in HCT116 but not in HeLa cells. Relative *hsa-miR-145* levels were determined by real-time RT-PCR. (**B**–**C**) Effects of serum starvation on *hSPOP* mRNA (**B**) and protein (**C**). In (**C**), a typical western blot is shown in the insert where C is for CM and S is SF. *p<0.05.

High levels of SPOP protein were also detected in the seminiferous tubule of the mouse testis at the site of late-spermatid stage of spermatogenesis (figure 1B). There are numerous reports on the ubiquitination of spermatid histones and on the crucial role of accurate ubiquitination in the spermatogenesis process in mammals (Baarends *et al.* 2000; Sutovsky *et al.* 2003; Laan *et al.* 2005). In more recent reports, further details in the (de)ubiquitination enzymes and their targets in the ubiquitination process in spermatogenesis have been defined (Nishito *et al.* 2006; Liu *et al.* 2007; Wright *et al.* 2007; Bao *et al.* 2010).

It was evident in our data that, in some of the tissues and cell lines analysed, the SPOP protein levels were in an inverse relationship with the *miR-145* levels (figures 2 and 3) supporting post-transcriptional regulation. Putative *miR-145* regulation was further substantiated by luciferase assays of deletion and mutation of the putative *miR-145* binding site and down-regulation of the endogenous SPOP levels by ectopic or serum starvation-induced over-expression of *miR-145* (figures 4 and 5). *miR-145* is a highly versatile miRNA that targets transcripts encoding for a wide array of proteins of diverse biological functions. Ample evidence supports a tumour suppressor role for *miR-145* through its mediation of cell growth, invasion and metastasis (Sachdeva and Mo 2010; Li *et al.* 2011;Xu *et al.* 2012). *miR-145* has further been shown to suppress expression of well-defined cellular reprogramming factors, such as Oct4 and c-Myc, in the induction of pluripotency and in subsequent differentiation of the induced pluripotent stem cells (Sun *et al.* 2010).

In recent years, components of the ubiquitination process have increasingly been shown to be under miRNA regulation. In cardiac hypertrophy, the ubiquitin-conjugating enzymes, Ube2i and Ube2gi, are up-regulated by *miR-199a* (Haghikia *et al.* 2011). The *let-7* miRNA family has been shown to regulate the fine-tuning and coordinated expression of subunits of the COP9 signalosome complex, which controls protein degradation via the ubiquitination process (Leppert *et al.* 2011). In a study on human dendritic cell development, Kip1 ubiquitination-promoting complex 1 was shown to be targeted by *miR-155* contributing to monocyte differentiation into dendritic cells (Lu *et al.* 2011). Our finding of SPOP, a ubiquitin ligase, being regulated by *miR-145* further echoes involvement of miRNA in regulation the ubiquitination process.

The main finding of this study is post-transcriptional regulation of *SPOP* expression by a miRNA, namely *miR-145*. It is noted that the mutational analysis of the putative miR-145 binding site did not clearly indicate significant effects on the luciferase activities (figure 5), which may be indicative of the possible presence of other endogenous negative regulators in HCT116 cells that may have made such mutational analysis difficult to observe. Our bioinformatics analysis also clearly predicted the presence of at least two other putative binding sites for the *miR-548* and *miR-106* families both located upstream of the *miR-145* binding sites (data not shown). It remains to be established if *miR-145* acts in synergy with either or both *miR-548* and *miR-106*. Demonstration of synergism in subsequent studies would explain the limited extents of putative regulation by *miR-145* reported here, and would also establish that *SPOP* regulation is a complex affair involving multiple players.

Acknowledgements

This work was supported in part by a grant (NSC-101-2313-B-034-003) from the National Science Council (Taiwan) to CJH, and by a University Tunku Abdul Rahman intramural grant 6200/C39 to KBC.

References

Baarends WM, van der Laan R and Grootegoed JA 2000 Specific aspects of the ubiquitin system in spermatogenesis. *J. Endocrinol. Invest.* **23** 597–604

Bao J, Zhang J, Zheng H, Xu C and Yan W 2010 UBQLN1 interacts with SPEM1 and participates in spermiogenesis. *Mol. Cell. Endocrinol.* **327** 89–97

Berger MF, Lawrence MS, Demichelis F, Drier Y, Cibulskis K, Sivachenko AY, Sboner A, Esgueva R, *et al.* 2011 The genomic complexity of primary human prostate cancer. *Nature* **470** 214–220

Betel D, Wilson M, Gabow A, Marks DS and Sander C 2008 The microRNA.org resource: targets and expression. *Nucleic Acids Res.* **36** D149–153

Bunce MW, Boronenkov IV and Anderson RA 2008 Coordinated activation of the nuclear ubiquitin ligase Cul3-SPOP by the generation of phosphatidylinositol 5-phosphate. *J. Biol. Chem.* **283** 8678–8686

Byun B, Tak H and Joe CO 2007 BTB/POZ domain of speckle-type POZ protein (SPOP) confers proapoptotic function in HeLa cells. *Biofactors* **31** 165–169

Choo KB, Hsu MC, Tsai YH, Lin WY and Huang CJ 2011 Nuclear factor kappa B and tumor necrosis factor-alpha modulation of transcription of the mouse testis- and pre-implantation development-specific Rnf33/Trim60 gene. *FEBS J.* **278** 837–850

Choo KB, Chuang TJ, Lin WY, Chang CM, Tsai YH and Huang CJ 2010 Evolutionary expansion of SPOP and associated TD/POZ gene family: impact of evolutionary route on gene expression pattern. *Gene* **460** 39–47

Claiborn KC, Sachdeva MM, Cannon CE, Groff DN, Singer JD and Stoffers DA 2010 Pcif1 modulates Pdx1 protein stability and pancreatic beta cell function and survival in mice. *J. Clin. Invest.* **120** 3713–3721

Friedman RC, Farh KK, Burge CB and Bartel DP 2009 Most mammalian mRNAs are conserved targets of microRNAs. *Genome Res.* **19** 92–105

Haghikia A, *et al.* 2011 Signal transducer and activator of transcription 3-mediated regulation of miR-199a-5p links cardiomyocyte and endothelial cell function in the heart: a key role for ubiquitin-conjugating enzymes. *Eur. Heart J.* **32** 1287–1297

Hernandez-Munoz I, Lund AH, van der Stoop P, Boutsma E, Muijrers I, Verhoeven E, Nusinow DA, Panning B, *et al.* 2005 Stable X chromosome inactivation involves the PRC1 Polycomb complex and requires histone MACROH2A1 and the CULLIN3/SPOP ubiquitin E3 ligase. *Proc. Natl. Acad. Sci. USA* **102** 7635–7640

Huang CJ, Wu SC and Choo KB 2005a Transcriptional modulation of the pre-implantation embryo-specific Rnf35 gene by the Y-box protein NF-Y/CBF. *Biochem. J.* **387** 367–375

Huang CJ, Huang CC and Chang CC 2012 Association of the testis-specific TRIM/RBCC protein RNF33/TRIM60 with the cytoplasmic motor proteins KIF3A and KIF3B. *Mol. Cell. Biochem.* **360** 121–131

Huang CJ, Chang JG, Wu SC and Choo KB 2005b Negative transcriptional modulation and silencing of the bi-exonic Rnf35 gene in the preimplantation embryo. Binding of the CCAAT-displacement protein/Cux to the untranslated exon 1 sequence. *J. Biol. Chem.* **280** 30681–30688

Huang CJ, Lin WY, Chang CM and Choo KB 2009 Transcription of the rat testis-specific Rtdpoz-T1 and -T2 retrogenes during embryo development: co-transcription and frequent exonisation of transposable element sequences. *BMC Mol. Biol.* **10** 74.

Huang CJ, Chen CY, Chen HH, Tsai SF and Choo KB 2004 TDPOZ, a family of bipartite animal and plant proteins that contain the TRAF (TD) and POZ/BTB domains. *Gene* **324** 117–127

Huang Q and Figueiredo-Pereira ME 2010 Ubiquitin/proteasome pathway impairment in neurodegeneration: therapeutic implications. *Apoptosis* **15** 1292–1311

Jennewein C, von Knethen A, Schmid T and Brune B 2010 MicroRNA-27b contributes to lipopolysaccharide-mediated peroxisome proliferator-activated receptor gamma (PPARgamma) mRNA destabilization. *J. Biol. Chem.* **285** 11846–11853

Kan Z, *et al.* 2010 Diverse somatic mutation patterns and pathway alterations in human cancers. *Nature* **466** 869–873

Krek A, Grün D, Poy MN, Wolf R, Rosenberg L, Epstein EJ, MacMenamin P, da Piedade I, *et al.* 2005 Combinatorial microRNA target predictions. *Nat. Genet.* **37** 495–500.

Kwon JE, La M, Oh KH, Oh YM, Kim GR, Seol JH, Baek SH, Chiba T, *et al.* 2006 BTB domain-containing speckle-type POZ protein (SPOP) serves as an adaptor of Daxx for ubiquitination by Cul3-based ubiquitin ligase. *J. Biol. Chem.* **281** 12664–12672

Laan R, Baarends WM, Wassenaar E, Roest HP, Hoeijmakers JH and Grootegoed JA 2005 Expression and possible functions of DNA lesion bypass proteins in spermatogenesis. *Int. J. Androl.* **28** 1–5

Leppert U, Henke W, Huang X, Muller JM, Dubiel W. 2011 Post-transcriptional fine-tuning of COP9 signalosome subunit biosynthesis is regulated by the c-Myc/Lin28B/let-7 pathway. *J. Mol. Biol.* **409** 710–721

Li C, Ao J, Fu J, Lee DF, Xu J, Lonard D and O'Malley BW 2011 Tumor-suppressor role for the SPOP ubiquitin ligase in signal-dependent proteolysis of the oncogenic co-activator SRC-3/AIB1. *Oncogene* **30** 4350–4364

Liao Y, Du X and Lonnerdal B 2010 miR-214 regulates lactoferrin expression and pro-apoptotic function in mammary epithelial cells. *J. Nutr.* **140** 1552–1556

Liu A, Desai BM and Stoffers DA 2004 Identification of PCIF1, a POZ domain protein that inhibits PDX-1 (MODY4) transcriptional activity. *Mol. Cell. Biol.* **24** 4372–4383

Liu A, Oliver-Krasinski J and Stoffers DA 2006 Two conserved domains in PCIF1 mediate interaction with pancreatic transcription factor PDX-1. *FEBS Lett.* **580** 6701–6706

Liu J, Ghanim M, Xue L, Brown CD, Iossifov I, Angeletti C, Hua S, Nègre N, *et al.* 2009 Analysis of Drosophila segmentation network identifies a JNK pathway factor overexpressed in kidney cancer. *Science* **323** 1218–1222

Liu Z, Miao D, Xia Q, Hermo L and Wing SS 2007 Regulated expression of the ubiquitin protein ligase, E3(Histone)/LASU1/Mule/ARF-BP1/HUWE1, during spermatogenesis. *Dev. Dyn.* **236** 2889–2898

Lu C, Huang X, Zhang X, Roensch K, Cao Q, Nakayama KI, Blazar BR, Zeng Y, *et al.* 2011 miR-221 and miR-155 regulate human dendritic cell development, apoptosis, and IL-12 production through targeting of p27kip1, KPC1, and SOCS-1. *Blood* **117** 4293–4303

Matsuda N and Tanaka K 2010 Does impairment of the ubiquitin-proteasome system or the autophagy-lysosome pathway predispose individuals to neurodegenerative disorders such as Parkinson's disease? *J. Alzheimers Dis.* **19** 1–9

Moriyoshi K, Iijima K, Fujii H, Ito H, Cho Y, Nakanishi S. 2004. Seven in absentia homolog 1A mediates ubiquitination and degradation of group 1 metabotropic glutamate receptors. *Proc Natl Acad Sci USA* **101** 8614–8619

Nishito Y, Hasegawa M, Inohara N and Nunez G 2006 MEX is a testis-specific E3 ubiquitin ligase that promotes death receptor-induced apoptosis. *Biochem. J.* **396** 411–417

Sachdeva M and Mo YY 2010 miR-145-mediated suppression of cell growth, invasion and metastasis. *Am. J. Transl. Res.* **2** 170–180

Sachdeva M, Zhu S, Wu F, Wu H, Walia V, Kumar S, Elble R, Watabe K, *et al.* 2009 p53 represses c-Myc through induction of the tumor suppressor miR-145. *Proc. Natl. Acad. Sci. USA* **106** 3207–3212

Sun X, Fu X, Han W, Zhao Y and Liu H 2010 Can controlled cellular reprogramming be achieved using microRNAs? *Ageing Res. Rev.* **9** 475–483

Sutovsky P, Turner RM, Hameed S and Sutovsky M 2003 Differential ubiquitination of stallion sperm proteins: possible implications for infertility and reproductive seasonality. *Biol. Reprod.* **68** 688–698

Takahashi I, Kameoka Y and Hashimoto K 2002 MacroH2A1.2 binds the nuclear protein Spop. *Biochim. Biophys. Acta.* **1591** 63–68

Wang M, *et al.* 2010 Essential role of the unfolded protein response regulator GRP78/BiP in protection from neuronal apoptosis. *Cell Death Differ.* **17** 488–498

Wright A, Reiley WW, Chang M, Jin W, Lee AJ, Zhang M and Sun SC 2007 Regulation of early wave of germ cell apoptosis and spermatogenesis by deubiquitinating enzyme CYLD. *Dev. Cell* **13** 705–716

Xu Q, Liu LZ, Qian X, Chen Q, Jiang Y, Li D, Lai L and Jiang BH 2012 MiR-145 directly targets p70S6K1 in cancer cells to inhibit tumor growth and angiogenesis. *Nucleic Acids Res.* **40** 761–774

MS received 01 October 2013; accepted 02 April 2014

Corresponding editor: SEYED E HASNAIN